Highly Efficient FRET from a Single Nitrogen-Vacancy Center in Nanodiamonds to a Single Organic Molecule

Julia Tisler,[†,*] Rolf Reuter,[†] Anke Lämmle,[†] Fedor Jelezko,[‡] Gopalakrishnan Balasubramanian,[§] Philip R. Hemmer,[⊥] Friedemann Reinhard,[†] and Jörg Wrachtrup[†]

[†]Institute of Physics, University of Stuttgart, Stuttgart, Germany, [‡]Institute for Quantum Optics, University of Ulm, Ulm, Germany, [§]Max Planck Institute for Biophysical Chemistry, Göttingen, Germany, and [⊥]Texas A&M University, College Station, Texas

ABSTRACT We show highly efficient fluorescence resonance energy transfer (FRET) between negatively charged nitrogen-vacancy (NV) centers in diamond as donor and dye molecules as acceptor, respectively. The energy transfer efficiency is 86% with particles of 20 nm in size. Calculated and experimentally measured energy transfer efficiencies are in excellent agreement. Owing to the small size of the nanocrystals and careful surface preparation, energy transfer between a single nitrogen-vacancy center and a single quencher was identified by the stepwise change of energy transfer efficiencies due to bleaching of single acceptor molecules. Our studies pave the way toward FRET-based scanning probe techniques using single NV donors.

KEYWORDS: nitrogen-vacancy center · black hole quencher · DY781 · fluorescence resonance energy transfer · single molecule · scanning FRET microscope · fluorescent nanodiamond

The ever-increasing demand for detailed knowledge of structure and dynamics of complex materials has led to the development of a diverse set of local probes for fluorescence-based microscopy techniques. Initially dominated by organic molecular probes, metallic and semiconducting nanostructures such as quantum dots (QDs) meanwhile play an important role.[1] Recently nanodiamonds have been discussed as a novel nanomaterial that may be used as ideal nanosensors and even drug carriers.[2] This prospect arises from the fact that nanodiamonds can be doped with a variety of defects with extraordinary properties. One particularly prominent example is the negatively charged nitrogen-vacancy (NV) center. In different scientific areas such as nanoscale magnetometry,[3,4] quantum optics,[5−7] and biophysics[8] the nitrogen-vacancy center became an interesting system of research. Matchless photostability,[1] magnetic resonance at room temperature[9] combined with chemical inertness, photoswitching,[10] and excellent biocompatibility[2] have put nanodiamonds with nitrogen-vacancy centers at the forefront of novel fluorescent probes. It was reported that fluorescent nanodiamonds with a NV center can achieve sizes of 4 nm[11] through progress in irradiation and milling. Recent research showed that even these very small nanodiamonds retain their optical and spin properties.[12] On the basis of these findings the NV center in diamond appears as an ideal candidate as a nanosensor for novel high-resolution imaging methods. Although there is significant progress in research using fluorescent nanodiamonds for sensing applications, there are no interactions with single molecules reported so far. In this work, we show fluorescence resonance energy transfer (FRET) between single negatively charged nitrogen-vacancy centers and single quencher molecules (Black Hole Quencher 3) as well as dye molecules (DY781).

FRET has become an efficient and important tool for studying biological phenomena.[13] It is a nonradiative dipole−dipole interaction between two molecules. If these molecules are in close proximity, one molecule—the donor—transfers its energy to the other molecule—the acceptor. Therefore, the fluorescence lifetime and intensity of the donor decrease. The photostability of biomarkers has become an issue of ongoing scientific work and is of utmost importance especially for FRET. Organic dyes and fluorescent proteins that are mainly used as fluorophores in biology[14] provide low photostability and show blinking behavior and thus are limited for long-term *in vivo* or *in vitro* studies.[15] Particularly for single-molecule studies this often hampers in-depth investigations. For this reason other candidate labels such as

* Address correspondence to j.tisler@physik.uni-stuttgart.de.

Received for review June 9, 2011 and accepted September 7, 2011.

Published online September 07, 2011
10.1021/nn2021259

quantum dots meanwhile have their firm place in biological research. QDs are brighter and more photostable than organic molecules or proteins[16] and are also used as donors in FRET experiments.[17] Fluorescent nanodiamonds with particle sizes being on the order of the smallest energy transfer distances[18] together with their inherent photostability potentially are ideal candidates as FRET labels.

Recently, FRET between several NVs and several IRDye molecules with an energy transfer efficiency of 7%[19] has been reported. Here we describe energy transfer between single NV centers and *single* quencher molecules with an energy transfer efficiency of 95%.

RESULTS AND DISCUSSION

For the present study two different samples of labeled nanodiamonds are prepared: one sample with dye (DY781-NHS) covalently linked by amide bonds to the surface of amino-silanized nanodiamonds and another with Black Hole Quencher (BHQ3-NH_2) strongly attached to the surface by electrostatic interaction with the negatively charged nanodiamond surface at pH 6. In order to covalently bind the DY781 to the surface of the nanodiamonds, an oxidizing acid treatment to remove sp^2 carbon was followed by borane reduction to create hydroxyl groups and also to stabilize the NV^- charge state.[20−23] An aminosilanization treatment of the nanodiamond surface was carried out, and the FRET acceptor was bound using its *N*-hydroxysuccinimide (NHS) ester derivative.[24]

The DY781 sample showed fast bleaching of the dye molecules, and as a result of that, a different sample using BHQ as FRET acceptor was prepared. The BHQ was attached to the naodiamond surface *via* adsorption, and this resulted in a higher coverage rate than DY781.

Zeta potential measurements show a value of −40 mV at pH 7, indicating a high surface coverage with negative charges after the oxidizing treatment. As a result, the positively charged BHQ adsorbs strongly by electrostatic interaction. The treated nanodiamonds were then spin-coated on a glass slide.

For the experiment we used a combination of an atomic force microscope and a confocal microscope with fluorescence lifetime imaging (FLIM) capability. This allows for simultaneous measurement of the topography, confocal image, and lifetime image of the same area. We used a pulsed laser with a wavelength of $\lambda = 532$ nm for excitation and two filters for detecting the fluorescence of the NV center and of the dye (FRET signal). The bandpass filter from 650 to 750 nm separates NV^0 from NV^-. In addition, the spectrum of NV^0 is shifted to the blue so that the FRET efficiency is very low due to the small overlap integral between NV^0 and BHQ. The NV center acts as a donor for both quencher and dye. To confirm single NV centers, autocorrelation curves were recorded (data not shown). Two scans (before and after bleaching of the acceptor molecules) were performed for every investigated sample area, and fluorescence lifetime and intensity data of the NV center were recorded each time. After the first scan, the dye molecules on the surface of the nanodiamonds were bleached by illuminating every particle with high laser power. The energy transfer efficiency was calculated by comparing lifetime and intensity data of the NV center before and after bleaching of the acceptor molecules.

In a first step the adsorption of dye molecules on the surface of nanodiamonds was confirmed with co-localization microscopy (Figure 1a). When comparing images where dye fluorescence is measured (Figure 1b) with those where NV fluorescence was carried out (Figure 1c), the NV channel (red) and the dye channel (green) nicely co-localize, indicating attachment of dyes on the surface (Figure 1a). It was found that DY781 bleaches very fast (as compared to the BHQ3). Nevertheless, we were able to detect DY781 fluorescence (Figure 1b) and hence a decrease in NV lifetime as well. Also in this case, on bleaching of DY781, only the signal of the NV center remains with a longer fluorescence lifetime (Figure 1c). The observed energy transfer furthermore confirms attachment of the dye on the nanodiamond surface.

The NV center emission ranges from 600 to 750 nm[25] and overlaps with the absorption maximum of DY781 at 783 nm (see Figure 1g). Using eq 1 we calculated the Förster radius between the NV center and DY781 to be 3.8 nm.

$$R_0 = 0.211(\kappa^2 n^{-4} Q_D J(\lambda))^{1/6} \quad (1)$$

κ is the orientation factor, which is assumed to be $\kappa^2 = 2/3$ for an average orientation factor. n is the refractive index (2.4 for diamond), and Q_D the quantum efficiency, with $Q_D = 0.3$. $J(\lambda)$ is the spectral overlap between the emission spectra of the NV center and the absorption spectra of the acceptor.

Figure 1d and e show FLIM of a sample with nanodiamonds covered with BHQ before and after bleaching. The fluorescence of the NV center and intensity as well as lifetime increased, after the quencher molecules have been bleached, which clearly indicates FRET.

To confirm this in a quantitative manner, we calculated the energy transfer efficiency using the recorded lifetime and intensity of the NV center before and after bleaching of the quencher. For a FRET process the efficiency calculated from fluorescence intensity and lifetime are correlated. To verify this, we calculated the energy transfer efficiency E:

$$E = 1 - \frac{\tau_{DA}}{\tau_D} = 1 - \frac{I_{DA}}{I_D} \quad (2)$$

Here τ_{da} and I_{da} are the lifetime and intensity between donor and acceptor before bleaching, and τ_d and I_d are

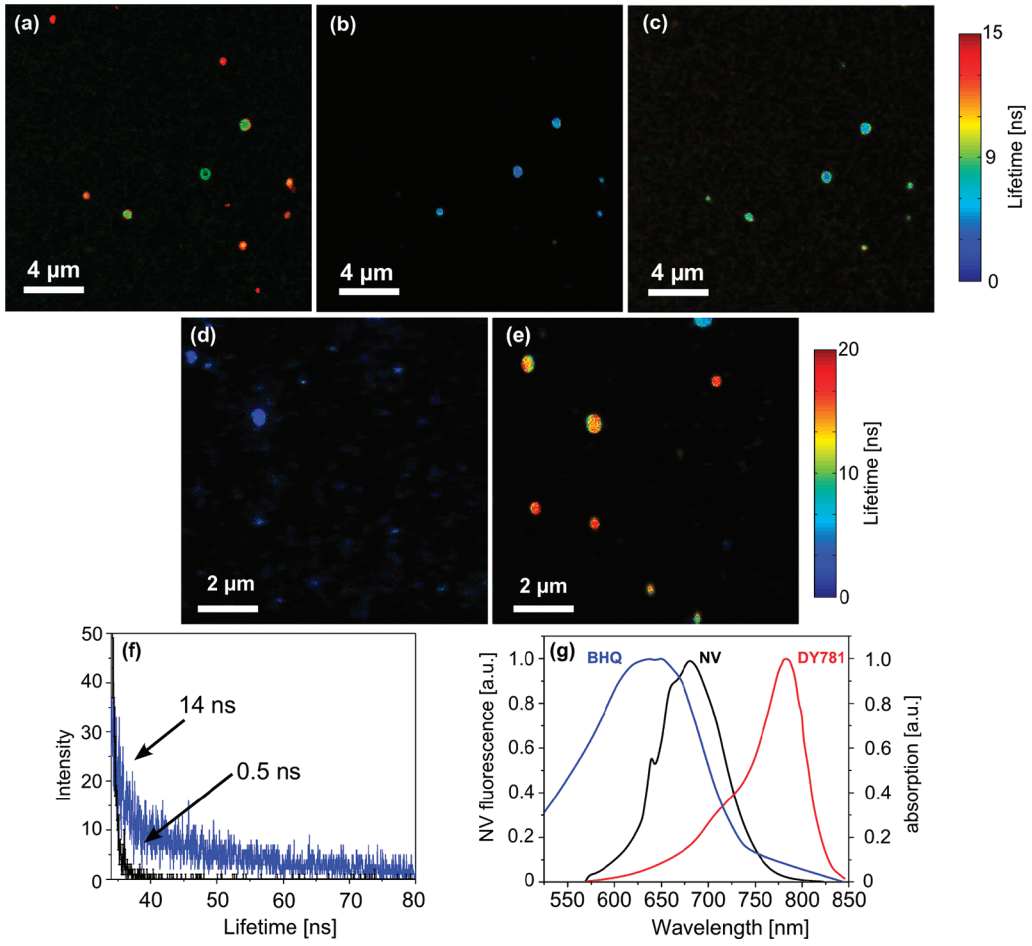

Figure 1. FLIM images of nanodiamonds with Black Hole Quencher and DY781. (a) Co-localization image of (b) and (c). (b) Image of DY781 attached to nanodiamonds. (c) Image of NV center fluorescence from the same nanodiamonds shown in (b). Nanodiamonds with BHQ before (d) and after (e) bleaching. In both cases the lifetime of the NV center was detected. Both lifetime and intensity increased. (f) Lifetime of nanodiamond before (black curve) and after bleaching (blue curve). Roughly 30% of all nanocrystals contained a NV center and were suitable for the experiments. (g) Overlap of the NV emission spectrum with the BHQ and DY781.

the lifetime and intensity of the donor (NV) after bleaching. After acceptor bleaching the NV lifetime increased to the average value of 16 ns, which is very close to an untreated nanodiamond.

The experimental data of the energy transfer efficiency are shown in Figure 2a. The energy transfer efficiency calculated from intensity is plotted *versus* energy transfer efficiency calculated from lifetime. The curve shows the expected theoretical result and fits approximately to the experimental data.

We also analyzed the dependence of the transfer efficiency on the nanodiamonds' size for 41 nanodiamonds (Figure 2c) and observed that, as expected, the FRET efficiency decreases for increasing size. We attribute this to the short range of the FRET interaction. The FRET transfer efficiency drops with the distance r between the NV and an acceptor dye as

$$E = \frac{{R_0}^6}{{R_0}^6 + r^6} \qquad (3)$$

where R_0 denotes the Förster radius. In a sufficiently large nanodiamond, a randomly placed NV center can have distances $r \gg R_0$ to every dye on the surface and, hence, show a low transfer efficiency.

On the other hand even for small distances between the NV center and dye molecule, $r < R_0$, an unfavorable orientation can result in a low transfer efficiency. To reproduce this effect, we have carried out a Monte Carlo simulation (Figure 2b) modeling an ensemble of 150 nanodiamonds for a given diameter. For each nanodiamond 200 dyes were randomly placed on the surface and their resulting FRET efficiency was computed for a single NV center, which was placed randomly inside the nanodiamond.

The transfer efficiency was evaluated as

$$E = \frac{1}{1 + \sum_{d \in dyes} \frac{{R_0}^6}{{r_d}^6}} \qquad (4)$$

with r_d denoting the distance between the NV and the dye. The Förster radius R_0 between NV and BHQ was calculated to be 3.6 nm. From this ensemble (dots in

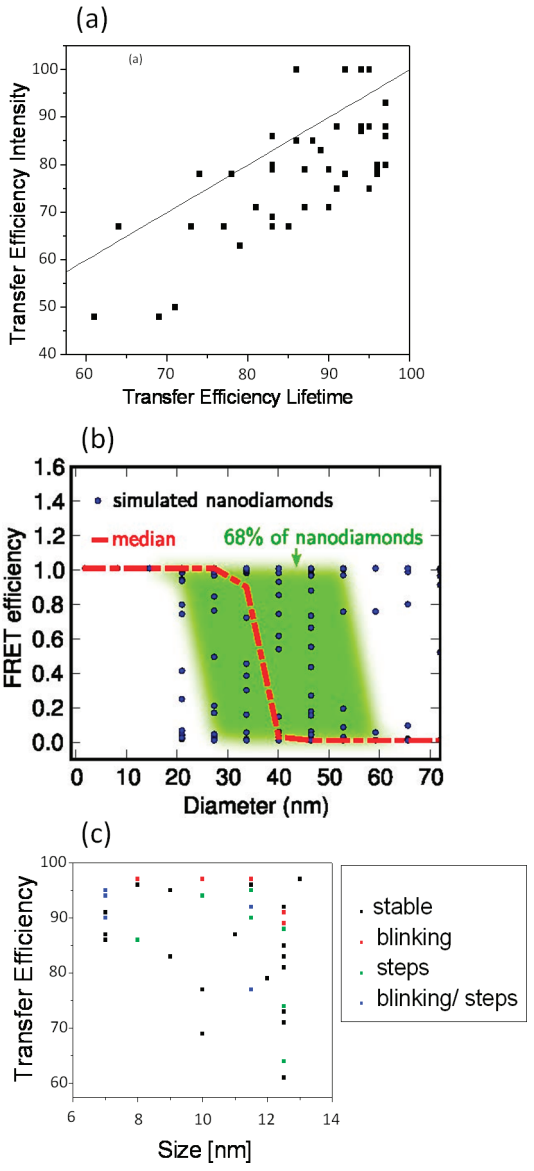

Figure 2. Energy transfer efficiency between NV center and BHQ. (a) Comparison between the transfer efficiency based on experimental lifetime and intensity data and the theoretical curve. (b) Theoretical FRET efficiency as a function of nanodiamond size. Every black point denotes a simulated nanodiamond. For each diameter an ensemble of nanodiamonds was simulated and used to compute the quenching efficiency's median (red) and standard deviation (green). (c) Experimental FRET efficiency as a function of the size of the nanodiamonds including indication for steps and blinking particles.

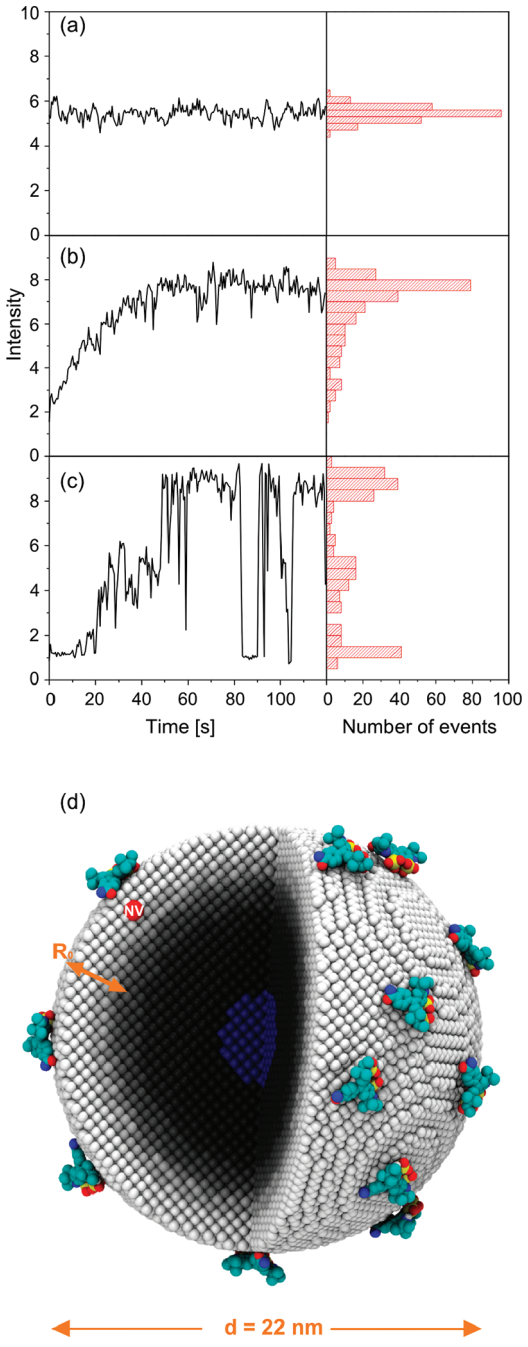

Figure 3. Intensity graphs of nanodiamonds with intensity histograms. (a) Intensity graph of a nanodiamond. (b) Intensity graph of a nanodiamond with BHQ during bleaching. The increase is continuous. (c) Intensity graph of a nanodiamond with BHQ. The increase shows steps and blinking indicating an interaction between two single molecules. (d) Nanodiamond with the NV center functionalized with dyes. Only within the Förster radius R_0 is the NV quenched (white area).[26]

Figure 2b) we computed the median (red line in Figure 2b) and the standard deviation (Figure 2b: green area) of the quenching efficiency. The entire procedure was repeated for 12 diameters between 2 and 70 nm.

This simulation (Figure 2b) indeed reproduces the essential features of the experiment (Figure 2c). For small nanodiamonds, the energy transfer efficiency is unity in the simulation and close to unity within the experimental error in the experiment. For sizes bigger than 20 nm in diameter nanodiamonds with a low FRET efficiency appear in the simulation as well as in the experiment. This diameter is much larger than the Förster radius of a single dye, which suggests that our preparation procedure indeed produced a high coverage as assumed in the parameters of the simulation.

More insight into the local environment of a center can be gained by recording time traces of the intensity and lifetime during the bleaching process that was measured for every NV center. These curves were acquired by illuminating every particle with high laser power. Therefore quencher molecules are progressively bleached, and the detected NV intensity as well as its lifetime increased proportionally to the remaining number of dye molecules on the surface. Figure 3 shows some examples of the intensity curves and the corresponding intensity histogram. The first example is a NV center without quencher and shows the well-known time trace without blinking or bleaching. In the following graphs there is a continuous increase in intensity, and in panel 3c the intensity increases in steps. The percentage increase of both lifetime and intensity was the same for all curves and was verified by

$$I\left(\frac{1}{k_2+k_3}\right) = a k_1 k_2 \frac{1}{k_2+k_3} \quad (5)$$

I is the intensity, a is a constant, k_1 is the excitation rate, k_2 is the fluorescing rate, and k_3 is the quenching rate. The lifetime τ can be expressed as $1/(k_2 + k_3)$. Equation 5 gives a relation between the quenched intensity and lifetime and shows that the percentage increase of lifetime and intensity was the same, indicating a real FRET signal as opposed to blinking caused by photoionization of the NV,[18] which usually does not shorten the lifetime.

Thirty-four percent of the particles showed steps (Figure 3c), while the rest showed a continuous increase in which finally all dye molecules were fully bleached (Figure 3b). Steps indicate an interaction between a single NV and a single quencher molecule that bleached, visible in a sudden increase in intensity and lifetime of the NV. Naively one might expect that all curves should show stepwise increase in intensity at least at the end, when almost all molecules on the surface have been bleached. In this case the NV center is within the Förster radius, R_0. Figure 3d shows a 22 nm diamond functionalized with dyes where the energy transfer efficiency is color coded. If the NV is in the white shell, it is close enough to the surface for FRET to an adsorbed molecule; if it is in the core (the blue area) and too far away from the surface, no quenching should appear. The volume of that core divided by the whole volume of the nanodiamond results in the probability of the quenched particles η, where we expect to see steps:

$$\eta = 1 - \frac{(r - R_0)^3}{r^3} \quad (6)$$

We estimate that 70% of the particles should show steps for an average size of 20 nm. The observation that this is not the case together with the observation that every particle showed quenching on the other hand is due to the high coverage of quencher molecules on the surface of the nanodiamonds. Many molecules are not in the range of the Förster radius, but the NV is close enough to the surface (black area) to be quenched by the high number of acceptors showing a continuous increase. This, on the other hand, can be used to estimate the number of molecules on the surface. The nanodiamond in Figure 3c shows two steps; that is, two molecules are within the Förster radius. The particle has a radius of 7 nm. If one divides the surface of a nanodiamond with radius 7 nm by the area that has two quencher molecules, about 30 molecules on the surface can be estimated.

For some NVs the curves show a blinking behavior (see Figure 3c). As shown before, the NV center in diamond is stable. Also the reference sample showed only 4% of blinking NVs, compared to the sample with the treated nanodiamonds, where 26% showed such a behavior. The blinking was visible in the intensity as well as the lifetime curves. This suggests that the blinking is not caused by the NV but by the acceptor molecules. The acceptor molecule switches on and off before it is completely bleached. In Figure 2c the energy transfer efficiency as a function of the particle radius is shown with statistics of the nanodiamonds showing these effects. The figure shows that in some cases the steps are accompanied by blinking. Note that especially for the smallest particles of 7 nm in size this behavior is observed. Every particle measured with this radius showed steps and blinking. This is a further indication that blinking of NVs as observed in our case is a signature for FRET.

CONCLUSION

In conclusion we showed that we were able to functionalize diamond nanocrystals for covalent attachment of acceptor molecules on their surface. In some cases this causes strong interaction between a single NV center and a single quencher molecule with near unit FRET transfer efficiency between the NV and quencher molecule. Because the NV center in diamond provides several advantages such as photostability and biocompatibility, it is an ideal candidate for FRET investigations. Besides it was shown that nanocrystals can be produced down to sizes of 4 nm;[27] thus the nitrogen-vacancy center is a biomarker that can be used for FRET studies in biological applications. Finally the observed FRET efficiencies may foster developments of FRET microscopes based on single NV centers as donors, which would be truly novel devices.[28]

METHODS

The used nanodiamonds were irradiated with electrons and annealed as described previously.[12] The fluorescent defect centers containing diamond nanocrystals were oxidized in air at 480 °C for 12 h to selectively remove sp^2-bonded carbon, followed by cleaning in a mixture of concentrated nitric, sulfuric,

and perchloric acid in a volume ratio of 1:1:1. This cleaning step was done under reflux for 10 h with 30 min of sonification in an ultrasonic bath after each 2 h of reflux. Extensive rinsing with Milli-Q water led to a stable, clear, and brownish solution.

Experimental Setup. The experiment was performed using a home-built scanning confocal microscope combined with an AFM (MFP-3D Asylum Research). Nitrogen-vacancy defects were excited with a frequency doubled CW Nd:YAG laser (Coherent Compass) and for lifetime measurements with a Vanguard Quasi-CW DPSS laser (Newport Spectra-Physics) focused onto the sample with a high-NA objective (Olympus PlanAPO, NA51.35). Lunimescence light was collected by the same objective and filtered from the excitation light using a dichroic beamsplitter (640 DCXR, Chroma). Photon counting of the filtered light was performed using two avalanche photodiodes (SPQR-14, Perkin-Elmer). Fluorescence autocorrelation histograms were recorded using a fast multichannel analyzer (Fastcomtec, P7889). Fluorescence lifetime and the autocorrelation histograms were recorded using TCSPC electronics (PicoHarp 300, PicoQuant GmbH) together with a two-channel router controlled by SymPhoTime V 4.0 software.

Acknowledgment. This work was financially supported by the Volkswagenstiftung as well as the EU projects DINAMO as well as SQUTEC and Baden-Württemberg Stiftung through the projects Internationale Spitzenforschung II and Methoden für die Lebenswissenschaften. We thank Philip R. Hemmer for helpful comments on the manuscript, Roman Kolesov for experimental assistance, and Andrew Aird for help with the preparation of the figures and the manuscript.

REFERENCES AND NOTES

1. Michalet, X.; Pinaud, F. F.; Bentolila, L. A.; Tsay, J. M.; Doose, S.; Li, J. J.; Sundaresan, G.; Wu, A. M.; Gambhir, S. S.; Weiss, S. Quantum Dots for Live Cells, *in Vivo* Imaging, and Diagnostics. *Science* **2005**, *307*, 538–544.
2. Schrand, A. M.; Huang, H.; Carlson, C.; Schlager, J. J.; Ōsawa, E.; Hussain, S. M.; Dai, L. Are Diamond Nanoparticles Cytotoxic? *J Phys.Chem. B* **2007**, *111*, 2–7.
3. Balasubramanian, G.; Chan, I. Y.; Kolesov, R.; Al-Hmoud, M.; Tisler, J.; Shin, C.; Kim, C.; Wojcik, A.; Hemmer, P. R.; Krueger, A.; *et al.* Nanoscale Imaging Magnetometry with Diamond Spins under Ambient Conditions. *Nature* **2008**, *455*, 648–651.
4. Maze, J. R.; Stanwix, P. L.; Hodges, J. S.; Hong, S.; Taylor, J. M.; Cappellaro, P.; Jiang, L.; Dutt, M. V. G.; Togan, E.; Zibrov, A. S.; *et al.* Nanoscale Magnetic Sensing with an Individual Electronic Spin in Diamond. *Nature* **2008**, *455*, 644–647.
5. Beveratos, A.; Brouri, R.; Gacoin, T.; Poizat, J.-P.; Grangier, P. Nonclassical Radiation from Diamond Nanocrystals. *Phys. Rev. A* **2001**, *64*, 061802.
6. Kurtsiefer, C.; Mayer, S.; Zarda, P.; Weinfurter, H. Stable Solid-State Source of Single Photons. *Phys. Rev. Lett.* **2000**, *85*, 290.
7. Wu, E.; Jacques, V.; Zeng, H.; Grangier, P.; Treussart, F.; Roch, J.-F. Narrow-Band Single-Photon Emission in the Near Infrared for Quantum Key Distribution. *Opt. Express* **2006**, *14*, 1296–1303.
8. Chang, Y.-R.; Lee, H.-Y.; Chen, K.; Chang, C.-C.; Tsai, D.-S.; Fu, C.-C.; Lim, T.-S.; Tzeng, Y.-K.; Fang, C.-Y.; Han, C.-C.; *et al.* Mass Production and Dynamic Imaging of Fluorescent Nanodiamonds. *Nat. Nanotechnol.* **2008**, *3*, 284–288.
9. Gruber, A.; Dräbenstedt, A.; Tietz, C.; Fleury, L.; Wrachtrup, J.; Borczyskowski, C. von. Scanning Confocal Optical Microscopy and Magnetic Resonance on Single Defect Centers. *Science* **1997**, *276*, 2012–2014.
10. Han, K. Y.; Kim, S. K.; Eggeling, C.; Hell, S. W. Metastable Dark States Enable Ground State Depletion Microscopy of Nitrogen Vacancy Centers in Diamond with Diffraction-Unlimited Resolution. *Nano Lett.* **2010**, *10*, 3199–3203.
11. Boudou, J.-P.; Curmi, P. A.; Jelezko, F.; Wrachtrup, J.; Aubert, P.; Sennour, M.; Balasubramanian, G.; Reuter, R.; Thorel, A.; Gaffet, E. High Yield Fabrication of Fluorescent Nanodiamonds. *Nanotechnology* **2009**, *20*, 235602.
12. Tisler, J.; Balasubramanian, G.; Naydenov, B.; Kolesov, R.; Grotz, B.; Reuter, R.; Boudou, J.-P.; Curmi, P. A.; Sennour, M.; Thorel, A.; *et al.* Fluorescence and Spin Properties of Defects in Single Digit Nanodiamonds. *ACS Nano* **2009**, *3*, 1959–1965.
13. Lakowicz, J. R. *Principles of Fluorescence Spectroscopy*; Springer: Berlin, 2006.
14. Giepmans, B. N. G.; Adams, S. R.; Ellisman, M. H.; Tsien, R. Y. The Fluorescent Toolbox for Assessing Protein Location and Function. *Science* **2006**, *312*, 217–224.
15. Fu, C.-C.; Lee, H.-Y.; Chen, K.; Lim, T.-S.; Wu, H.-Y.; Lin, P.-K.; Wei, P.-K.; Tsao, P.-H.; Chang, H.-C.; Fann, W. Characterization and Application of Single Fluorescent Nanodiamonds as Cellular Biomarkers. *Proc. Natl. Acad. Sci. U. S. A.* **2007**, *104*, 727–732.
16. Pohl, A.; Gubarevich, T.; Lapina, V.; Appelhans, D.; Rödel, G.; Pompe, W.; Schreiber, J.; Opitz, J.; Mkandawire, M. Selective Targeting of Green Fluorescent Nanodiamond Conjugates to Mitochondria in HeLa Cells. *J. Biophotonics* **2009**, *2*, 596–606.
17. Rogach, A. L.; Klar, T. A.; Lupton, J. M.; Meijerink, A.; Feldmann, J. Energy Transfer with Semiconductor Nanocrystals. *J. Mater. Chem.* **2009**, *19*, 1208.
18. Bradac, C.; Gaebel, T.; Naidoo, N.; Sellars, M. J.; Twamley, J.; Brown, L. J.; Barnard, A. S.; Plakhotnik, T.; Zvyagin, A. V.; Rabeau, J. R. Observation and Control of Blinking Nitrogen-Vacancy Centres in Discrete Nanodiamonds. *Nat. Nanotechnol.* **2010**, *5*, 345–349.
19. Mohan, N.; Tzeng, Y.; Yang, L.; Chen, Y.; Hui, Y. Y.; Fang, C.; Chang, H. Sub-20-nm Fluorescent Nanodiamonds as Photostable Biolabels and Fluorescence Resonance Energy Transfer Donors. *Adv. Mater.* **2010**, *22*, 843–847.
20. Hauf, M. V.; Grotz, B.; Naydenov, B.; Dankerl, M.; Pezzagna, S.; Meijer, J.; Jelezko, F.; Wrachtrup, J.; Stutzmann, M.; Reinhard, F.; *et al.* Chemical Control of the Charge State of Nitrogen-Vacancy Centers in Diamond. *Phys. Rev. B* **2011**, *83*, 081304.
21. Fu, K.-M. C.; Santori, C.; Barclay, P. E.; Beausoleil, R. G. Conversion of Neutral Nitrogen-Vacancy Centers to Negatively Charged Nitrogen-Vacancy Centers through Selective Oxidation. *Appl. Phys. Lett.* **2010**, *96*, 121907.
22. Rondin, L.; Dantelle, G.; Slablab, A.; Grosshans, F.; Treussart, F.; Bergonzo, P.; Perruchas, S.; Gacoin, T.; Chaigneau, M.; Chang, H.-C.; *et al.* Surface-Induced Charge State Conversion of Nitrogen-Vacancy Defects in Nanodiamonds. *Phys. Rev. B* **2010**, *82*, 115449.
23. Petráková, V.; Nesládek, M.; Taylor, A.; Fendrych, F.; Cígler, P.; Ledvina, M.; Vacík, J.; Šturša, J.; Kučka, J. Luminescence Properties of Engineered Nitrogen Vacancy Centers in a Close Surface Proximity. *Phys. Status Solidi A* **2011**, 1–6.
24. Krueger, A.; Stegk, J.; Liang, Y.; Lu, L.; Jarre, G. Biotinylated Nanodiamond: Simple and Efficient Functionalization of Detonation Diamond. *Langmuir* **2008**, *24*, 4200–4204.
25. Gaebel, T.; Domhan, M.; Wittmann, C.; Popa, I.; Jelezko, F.; Rabeau, J.; Greentree, A.; Prawer, S.; Trajkov, E.; Hemmer, P. R.; Wrachtrup, J. Photochromism in Single Nitrogen-Vacancy Defect in Diamond. *Appl. Phys. B: Laser Opt.* **2005**, *82*, 243–246.
26. Humphrey, W.; Dalke, A.; Schulten, K. VMD: Visual Molecular Dynamics. *J. Mol. Graphics* **1996**, *14*, 33–38.
27. Morita, Y.; Takimoto, T.; Yamanaka, H.; Kumekawa, K.; Morino, S.; Aonuma, S.; Kimura, T.; Komatsu, N. A Facile and Scalable Process for Size-Controllable Separation of Nanodiamond Particles as Small as 4 nm. *Small* **2008**, *4*, 2154–2157.
28. Berman, G. P.; Chernobrod, B. M. Spin Microscope Based on Optically Detected Magnetic Resonance. *J. Appl. Phys.* **2005**, *97*, 014903.